Fuel 302 (2021) 121165

Contents lists available at ScienceDirect

Fuel

journal homepage: www.elsevier.com/locate/fuel

Full Length Article

Carbon dioxide absorption with aqueous amine solutions promoted by piperazine and 1-methylpiperazine in a rotating zigzag bed

Zhibang Liu [a], Arash Esmaeili [a], Hanxiao Zhang [a], Hao Xiao [a], Jimmy Yun [b,c], Lei Shao [a,*]

[a] Research Center of the Ministry of Education for High Gravity Engineering and Technology, Beijing University of Chemical Technology, Beijing 100029, China
[b] College of Chemical and Pharmaceutical Engineering, Hebei University of Science and Technology, Shijiazhuang, Hebei Province 050018, China
[c] School of Chemical Engineering, The University of New South Wales, Sydney, NSW 2052, Australia

ARTICLE INFO

Keywords:
Rotating zigzag bed
Carbon dioxide
Absorption efficiency
Blended aqueous amine solution
Gas-liquid mass transfer

ABSTRACT

In order to overcome the drawback of short liquid resistance time in rotating packed bed (RPB), a multi-stage rotating zigzag bed (RZB) was employed to enhance carbon dioxide (CO_2) absorption process with blended aqueous amine solutions containing diethylenetriamine (DETA) + piperazine (PZ) or DETA + 1-methylpiperazine (1-MPZ) as absorbents. The effects of different operating parameters on the CO_2 absorption efficiency, overall gas-phase volumetric mass transfer coefficient (K_Ga) and height of mass transfer unit in the RZB were investigated. Experimental results indicated that increase of the promoter concentration, lean solution flow rate and rotational speed were conducive to gas–liquid mass transfer and CO_2 absorption. It was found that both PZ and 1-MPZ were effective promoters, while PZ exhibited better performance. Meanwhile, comparison of CO_2 absorption performance between one stage and two stages revealed that two stages had higher CO_2 absorption efficiency due to extended residence time of absorbents and CO_2 in the RZB. A comparison with RPB demonstrated that the RZB could achieve higher mass transfer and CO_2 absorption efficiencies with smaller rotor volume and less absorbent consumption. The maximum CO_2 absorption efficiency and K_Ga reached 99.3% at a gas flow rate of 1.5 m^3/h and 7.43 kmol/kPa m^3 h at an inlet gas CO_2 concentration of 2% respectively in the RZB with DETA + PZ system, suggesting that RZB may be an effective device for CO_2 absorption.

1. Introduction

As a major contributor to the greenhouse effect, massive emission of carbon dioxide (CO_2) has a huge impact on the climate and environment, causing global warming, extreme weather and species extinction [1,2]. Data show that the CO_2 concentration in the atmosphere has risen substantially from 280 mL/m^3 to about 410 mL/m^3 since 1800 [3], and situation will only get worse if left unchecked. Therefore, the reduction of CO_2 emission is a very important task for the international community at present. Intergovernmental panel on climate change (IPCC) [4] aims to decrease CO_2 emission by 50% in 2050 relative to the standard of 1990. In order to achieve that, efficient CO_2 capture methods is indispensable. Different methods for CO_2 capture like absorption, adsorption, cryogenic distillation and membrane separation have been studied [5–7], in which post-combustion capture based on amine absorbent is the most mature process that has been successfully applied to petrochemical industry [8], and the development of efficient absorbents and devices are the key issues in this technology [9].

The conventional amine absorbents widely used for CO_2 absorption are monoethanolamine (MEA) and N-methyldiethanolamine (MDEA). MEA has high CO_2 absorption rate but low capacity and high regeneration energy [10,11]. On the contrary, although MDEA have the advantage of large capacity and low regeneration energy, its CO_2 absorption performance is restricted by low CO_2 absorption rate of MDEA [12]. Thus it is difficult to accomplish high CO_2 absorption rate, low regeneration energy consumption and large CO_2 loading capacity simultaneously for conventional alkanolamines [13].

Many new absorbents have been developed in recent years. Due to containing several functional amine groups, polyamines, such as diethylenetriamine (DETA) [14], triethylenetetramine (TETA) [15] and 2-((2-aminoethyl)amino)ethanol (AEEA) [16], usually have better performance on CO_2 absorption. DETA has a high CO_2 absorption rate because there are three amine groups in its molecular structure [17]. The CO_2 absorption rate of DETA is much faster than that of MEA [18]. A comparison of the CO_2 absorption performance between DETA and MEA in a packed column reveals that DETA has a significantly higher overall gas-phase volumetric mass-transfer coefficient than that of MEA [19].

* Corresponding author at: P.O. Box 35, No. 15 Bei San Huan Dong Road, Beijing 100029, China.
E-mail address: shaol@mail.buct.edu.cn (L. Shao).

https://doi.org/10.1016/j.fuel.2021.121165
Received 17 January 2021; Received in revised form 25 May 2021; Accepted 29 May 2021
Available online 10 June 2021

Nomenclature

C_{CO2}	CO_2 concentration in gas phase (%)
C_{Amine}	total amine concentration (wt%)
C_{DETA}	DETA concentration (wt%)
$C_{PZ/1\text{-}MPZ}$	PZ or 1-MPZ concentration (wt%)
G	inlet gas flow rate (m^3/h)
G'	inlet gas flow rate without dissolution and reaction (kmol/h)
H	axial length of rotor (m)
HTU	height of mass transfer unit (m)
k_{app}	apparent reaction rate constant (1/s)
k_{Am}	reaction rate constant contributed by amine (m^6/$kmol^2$ s)
k_{H2O}	reaction rate constant contributed by H_2O (m^6/$kmol^2$ s)
K_Ga	overall gas-phase volumetric mass transfer coefficient (kmol/kPa m^3 h)
L	lean solution flow rate (L/h)
m	phase equilibrium constant
$N_{CO2}a$	CO_2 absorption rate (kmol/m^3 h)
N	rotational speed of RZB (rpm)
NTU	number of mass-transfer unit
P	gas phase pressure (kPa)
r_i	inner radius of rotor (m)
r_o	outer radius of rotor (m)
T	lean solution temperature (°C)
$T_{inlet\ gas}$	inlet gas temperature (°C)
x_{CO2}	CO_2 concentration in liquid phase (mol/L)
y	molar concentration fraction of a component in gas phase (%)
y^*	equilibrium molar concentration fraction of a component in gas phase (%)
y_{CO2}	molar concentration fraction of CO_2 in gas phase (%)
$y_{CO2}{}^*$	equilibrium molar concentration fraction of CO_2 in gas phase (%)
$y_{CO2\text{-}in}$	molar concentration fraction of CO_2 in gas phase at gas inlet of RZB (%)
$y_{CO2\text{-}out}$	molar concentration fraction of CO_2 in gas phase at gas outlet of RZB (%)
α	CO_2 loading of absorbent (mol/mol)
η	CO_2 absorption efficiency (%)

Besides, DETA has larger CO_2 loading capacity and lower regeneration heat duty than MEA [20,21]. Moreover, CO_2 absorption rate and capacity of DETA exceeds those of other polyamines like TETA, tetraethylenepentamine (TEPA) and AEEA because DETA has more amine groups per unit weight [22,23]. At the same time, the lower viscosity and corrosiveness of DETA are more conducive to CO_2 absorption compared with other polyamines [23]. DETA also owns lower activation energy, higher boiling point, and lower vapor pressure than MEA [18,24], thereby exhibiting good CO_2 absorption performance.

In addition, use of blended absorbents is also an effective method to overcome the drawbacks of conventional amines and improve the CO_2 absorption performance by taking advantage of each absorbent [13,23]. As an efficient promoter in CO_2 absorption, DETA is usually employed to enhance CO_2 absorption effect of amines [25]. Previous studies revealed that the absorption rate, cyclic capacity, and desorption rate of 2-Amino-2-methyl-1-propanol (AMP) + DETA and AMP + MDEA + DETA absorbents were higher than those of MEA, while the absorption heat of AMP + DETA and AMP + MDEA + DETA absorbents was much lower than that of MEA [17,26]. CO_2 absorption performance of the amine absorbents can be improved by promoters such as piperazine (PZ) and its derivatives because of their fast CO_2 absorption rate [27,28]. The CO_2 absorption rate of PZ is higher than that of most amines [29], and thus PZ has been added into MEA, MDEA, DETA, AMP as a promoter to enhance CO_2 absorption rate of the blended amine absorbents [30–33]. DETA + PZ absorbent has shown not only higher CO_2 absorption rate, but also greater absorption capacity and lower regeneration energy consumption compared to MEA, confirming that DETA + PZ absorbent is a competitive CO_2 absorbent which can bring economic benefits in industrial applications when replacing MEA solution [23]. 1-methylpiperazine (1-MPZ) is a PZ derivative with a similar cyclic structure of PZ [34]. 1-MPZ also has a similar absorption rate with PZ because methyl group of 1-MPZ increases the reaction rate with its electron donor effect to the nitrogen atom [35,36]. A comparison of CO_2 absorption performance between 1-MPZ and PZ in a wetted wall column shows that liquid film mass transfer coefficient of 1-MPZ is similar to that of PZ [37]. Meanwhile, 1-MPZ has lower CO_2 absorption heat and higher cyclic capacity than PZ [35,38]. Moreover, 1-MPZ has a higher solubility in water relative to PZ, which tends to crystallize easily and often blocks pipes and equipment because of its low solubility [39].

To enhance CO_2 absorption effect, devices with high gas–liquid mass transfer efficiency are preferred. Rotating packed bed (RPB) is such a device and has found applications in different fields, such as gas absorption [40,41], water treatment [42] and polymerization [43]. In the high-gravity environment simulated by the centrifugal force in RPB, liquid is dispersed into microsized films, filaments and droplets, and thus interphase mass transfer and micromixing can be improved significantly [44]. Meanwhile, RPB possesses the advantage of small volume as compared to conventional column device, which is conducive to reducing the investment in equipment [45]. To date, various amine absorbents including MEA [46], DETA [29], AEEA [47] and blended absorbents [30,48,49], have been used to absorb CO_2 in RPB, and better mass transfer performance and higher CO_2 absorption efficiency have been achieved in comparison to packed columns [29,47,49]. Therefore, the application of efficient absorbents for CO_2 absorption in RPB can not only enhance the CO_2 absorption performance but also reduce the size of device.

However, because the liquid residence time in RPB is very short (usually between 200 ms and 800 ms [50]) and the mass transfer resistance of CO_2-amine system primarily lies in liquid phase [51], it is difficult to further boost CO_2 absorption efficiency. Rotating zigzag bed (RZB) innovates the rotor structure of RPB by employing a zigzag channel to replace the stainless-steel wire mesh packing in RPB [52,53], and is successfully applied to stripping, distillation [40], extraction [54] and gas–liquid reaction [55,56]. Liquid can be repeatedly dispersed and coalesced and contacts with gas stream in the zigzag channel. The rotor with the novel structure increases the gas–liquid contact time and liquid holdup markedly in RZB [57], which is conducive to gas–liquid mass transfer. It was found that the liquid film mass transfer coefficient in the RZB rotor was about 2.5 times higher than that in the RPB rotor with the stainless steel wire mesh packing [56]. Meanwhile, compared with RPB, RZB does not require liquid distributor and static seal, which simplifies the device structure and improves the reliability. Moreover, it is easier to install the multi-stage rotor and achieve intermediate feed in RZB [52,53,58], leading to more convenient operation and more efficient mass transfer [59,60]. These features of RZB suggest that it has great potential for the intensification of CO_2 absorption processes controlled by liquid film.

In this work, an RZB was employed for the first time to intensify CO_2 absorption by aqueous amine solutions and the effects of different operating conditions on the CO_2 absorption efficiency, overall gas-phase volumetric mass transfer coefficient (K_Ga) and height of mass transfer unit (HTU) were studied. Furthermore, CO_2 absorption performance of the RZB in one stage and two stages was explored, and the performance of the RZB for CO_2 absorption was also compared with that of an RPB.

2. Experimental section

2.1. Materials

DETA and PZ with a purity of 99% and 1-MPZ with a purity of 98% were purchased from Shanghai Macklin Biochemical Co. Ltd., China. The structures of the amines selected for this study are shown in Fig. 1. Carbon dioxide (99.0%) were purchased from Beijing Shunanqite Gas Co. Ltd., China. Deionized water was used throughout all the experiments. All chemicals were used without further purification.

The total concentration of the blended amine of DETA with PZ or 1-MPZ was 30 wt% in this study, with the concentration of PZ or 1-MPZ varying in the range of 0-10 wt% and that of DETA in the range of 30-20 wt% accordingly.

2.2. Experimental apparatus and procedure

The structure of the RZB employed in this study is shown in Fig. 2. The RZB has two stages (including bottom stage and up stage) and its parameters are shown in Table 1. The RZB rotor of one stage consists of nine rotational perforated baffles mounted on the rotating disk and ten stationary baffles fixed on the stationary disk. The rotational and stationary baffles are configured alternately in the radial direction.

The outside of the RZB casing was wrapped up in an insulating layer to maintain a specified temperature of the reaction environment in the RZB, which was determined by detecting the temperature of the insulating layer with an infrared thermometer (F-380, Shenzhen Flank Electronic Co. Ltd.).

Fig. 3 shows the experimental setup for CO_2 absorption process in the RZB with aqueous amine solutions as absorbents. A liquid at an elevated temperature was pumped into the RZB to preheat the RZB to a preset temperature and then the input of the liquid was stopped. Afterwards, CO_2 and air were mixed in a gas tank and introduced into the RZB through the gas inlet at the bottom stage. When a specified inlet gas CO_2 concentration was reached, the 30 wt% blended amine absorbent with a preset temperature in the lean solution tank was introduced into the RZB via the intermediate liquid inlet (for one-stage runs) or the top liquid inlet (for two-stage runs).

Gas stream flowed inward from the outer periphery of the rotor, while liquid stream flowed outward through the zigzag channel of rotor. In the whole, CO_2 and aqueous amine solution contacted countercurrently in the rotor of the RZB [57], and finally gas and liquid streams left the RZB from the gas and liquid outlet, respectively. All experiments were conducted under atmosphere pressure, and experimental data were recorded when the reaction attained a steady state. The CO_2 concentration of gas phase in the inlet and outlet was detected by a portable infrared CO_2 analyzer (GXH-3010F, Beijing Huayun Analytical Instrument Institution Co. Ltd.). The CO_2 loading of aqueous amine solution was determined by detecting the volume of CO_2 produced from the amine solution via reaction with excess dilute H_2SO_4 [29].

Considering that the gas flow rate entering and leaving the RZB varies with chemical reaction, the CO_2 absorption efficiency (η) can be calculated by the following equation:

$$\eta = \left[1 - \frac{y_{CO_2-out}\left(1 - y_{CO_2-in}\right)}{y_{CO_2-in}\left(1 - y_{CO_2-out}\right)}\right] \times 100\% \quad (1)$$

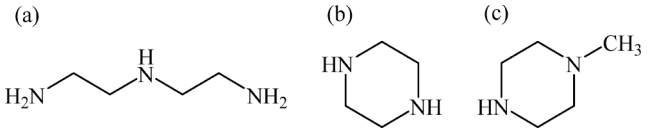

Fig. 1. Structures of amines in this study: (a) DETA; (b) PZ; (c) 1-MPZ.

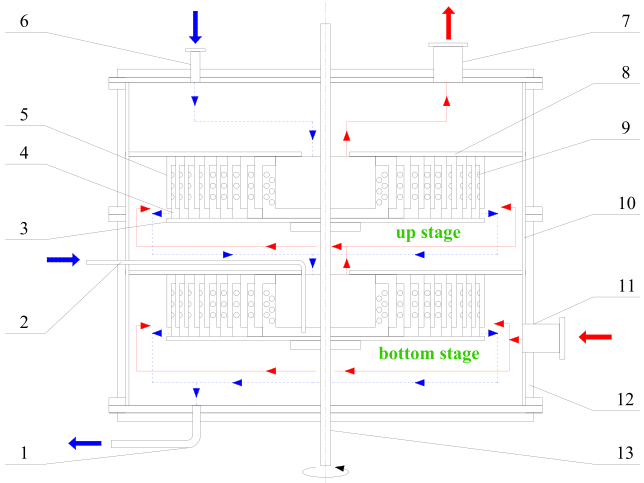

Fig. 2. Schematic diagram of RZB. (1) liquid outlet; (2) intermediate liquid inlet; (3) rotating disk; (4) rotational baffle; (5) stationary baffle; (6) top liquid inlet; (7) gas outlet; (8) stationary disk; (9) holes; (10) casing; (11) gas inlet; (12) insulating layer; (13) shaft. Red lines represent the gas flow; blue lines represent the liquid flow. (For interpretation of the references to colour in this figure legend, the reader is referred to the web version of this article.)

Table 1
Parameters of RZB.

Item	Value
Number of the stationary baffles	10
Number of the rotational baffles	9
Diameter of the stationary baffles (cm)	5.7, 8.1, 9.9, 11.4, 12.7, 14.0, 15.2, 16.3, 17.3, 18.3
Diameter of the rotational baffles (cm)	7.2, 9.0, 10.7, 12.2, 13.5, 14.7, 15.8, 16.8, 17.8
Inner diameter of the rotor (cm)	5.7
Outer diameter of the rotor (cm)	18.3
Axial length of the rotor (cm)	2.8
Volume of the rotor (cm^3)	665
Inner diameter of the casing (cm)	23.1
Diameter of the holes on the rotational baffles (mm)	2.1

2.3. Reactions of CO_2 in aqueous amine solution

The chemical interaction between CO_2 and aqueous amine solution includes several complex reversible reactions. The main reactions of the single amines (DETA, PZ and 1-MPZ) with CO_2 have been detailed as follows [17,34,35,61,62]:

$$DETAH^+ + H_2O \leftrightarrow DETA + H_3O^+ \quad (2)$$

$$DETA_2^{2+} + H_2O \leftrightarrow DETAH^+ + H_3O^+ \quad (3)$$

$$DETA_3^{3+} + H_2O \leftrightarrow DETA_2^{2+} + H_3O^+ \quad (4)$$

$$DETA + CO_2 + H_2O \leftrightarrow DETACOO^- + H_3O^+ \quad (5)$$

$$DETACOO^- + CO_2 + H_2O \leftrightarrow DETA(COO^-)_2 + H_3O^+ \quad (6)$$

$$DETA(COO^-)_2 + CO_2 + H_2O \leftrightarrow DETA(COO^-)_3 + H_3O^+ \quad (7)$$

$$DETAH_2^{2+}COO^- + H_2O \leftrightarrow DETAH^+COO^- + H_3O^+ \quad (8)$$

$$DETAH^+COO^- + H_2O \leftrightarrow DETACOO^- + H_3O^+ \quad (9)$$

$$DETAH^+(COO^-)_2 + H_2O \leftrightarrow DETA(COO^-)_2 + H_3O^+ \quad (10)$$

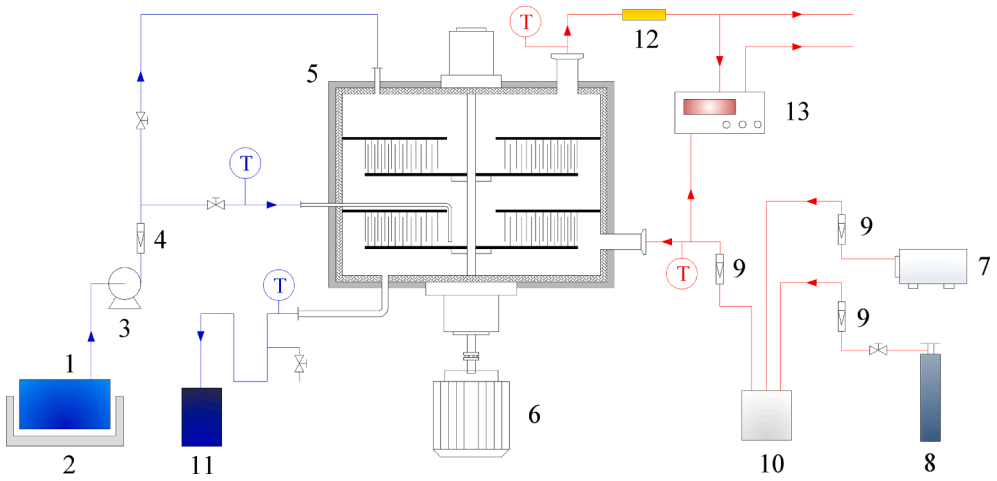

Fig. 3. Experimental setup for CO_2 absorption process. (1) lean solution tank; (2) thermostatic heater; (3) liquid pump; (4) liquid flowmeter; (5) RZB; (6) motor; (7) air compressor; (8) CO_2 cylinder; (9) gas flowmeter; (10) gas mixer; (11) rich solution tank; (12) dryer; (13) CO_2 analyzer.

$$DETACOO^- + H_2O \leftrightarrow DETA + HCO_3^- \quad (11)$$

$$DETA(COO^-)_2 + 2H_2O \leftrightarrow DETA + 2HCO_3^- \quad (12)$$

$$DETA(COO^-)_3 + 3H_2O \leftrightarrow DETA + 3HCO_3^- \quad (13)$$

$$PZ + H_2O \leftrightarrow PZH^+ + OH^- \quad (14)$$

$$PZH^+ + H_2O \leftrightarrow PZ + H_3O^+ \quad (15)$$

$$PZ + CO_2 + H_2O \leftrightarrow PZCOO^- + H_3O^+ \quad (16)$$

$$PZH^+ + CO_2 + H_2O \leftrightarrow H^+PZCOO^- + H_3O^+ \quad (17)$$

$$PZCOO^- + CO_2 + H_2O \leftrightarrow PZ(COO^-)_2 + H_3O^+ \quad (18)$$

$$H^+PZCOO^- + H_2O \leftrightarrow PZCOO^- + H_3O^+ \quad (19)$$

$$PZCOO^- + H_2O \leftrightarrow PZ + HCO_3^- \quad (20)$$

$$PZ(COO^-)_2 + 2H_2O \leftrightarrow PZ + 2HCO_3^- \quad (21)$$

$$1-MPZH^+ + H_2O \leftrightarrow 1-MPZ + H_3O^+ \quad (22)$$

$$1-MPZH^{2+} + H_2O \leftrightarrow 1-MPZH^+ + H_3O^+ \quad (23)$$

$$1-MPZ + CO_2 + H_2O \leftrightarrow 1-MPZCOO^- + H_3O^+ \quad (24)$$

$$H^+1-MPZCOO^- + H_2O \leftrightarrow 1-MPZCOO^- + H_3O^+ \quad (25)$$

$$1-MPZCOO^- + H_2O \leftrightarrow 1-MPZ + HCO_3^- \quad (26)$$

$$2H_2O \leftrightarrow H_3O^+ + OH^- \quad (27)$$

$$CO_2 + 2H_2O \leftrightarrow H_3O^+ + HCO_3^- \quad (28)$$

$$HCO_3^- + H_2O \leftrightarrow H_3O^+ + CO_3^{2-} \quad (29)$$

Eqs. (2)-(13) represent the reactions between CO_2 and aqueous DETA solution. DETA includes three amine groups which result in a complex CO_2-DETA reaction mechanism due to the presence of many species. Eqs. (14)-(21) represent the reactions between CO_2 and aqueous PZ solution, and Eqs. (22)-(26) represent the reactions between CO_2 and aqueous 1-MPZ solution. Ionization reactions for aqueous solution are represented in Eqs. (27)-(29). The reactions of these amine aqueous solutions with CO_2 include the following steps: protonation of amine, formation of carbamate, formation of protonated carbamate, hydrolysis of carbamate, dissociation of water, formation of bicarbonate and dissociation of bicarbonate.

Besides, in the blended aqueous DETA-based solution containing PZ or 1-MPZ, all the species (Eqs. (2)–(29)) are expected to be formed and possibly complement each other towards enhancing the CO_2–amine absorption reaction [31,33,61,63]. The reactions of CO_2 with amines are usually presumed to be pseudo-first-order reactions that can be expressed as Eqs. (30)-(31) [29,64]. Because PZ and 1-MPZ have a very fast reaction rate with CO_2 [29,37], adding PZ or 1-MPZ to DETA can improve the reaction rate of the blended absorbents.

$$-r_{CO_2} = k_{app}[CO_2] \quad (30)$$

$$k_{app} = \{k_{Am}[Am] + k_{H_2O}[H_2O]\}[Am] \quad (31)$$

2.4. Calculations of overall gas-phase volumetric mass transfer coefficient ($K_G a$) and height of mass transfer unit (HTU)

The rate of CO_2 absorption ($N_{CO_2}a$) into aqueous amine solution can be written as:

$$N_{CO_2}a = K_G a \times P\left(y_{co_2} - y^*_{co_2}\right) \quad (32)$$

where P is the total pressure, and y_{co_2} and $y^*_{co_2}$ are the molar concentration fraction and the equilibrium molar concentration fraction of CO_2 in the gas phase, respectively.

In the RZB, an infinitesimal mass transfer unit with an axial length of H can be seen as an annulus element with radial thickness of dr. It is assumed that the components in the gas flow stream except CO_2 neither dissolve in water nor react with amines, and the following expression can be obtained by mass conservation:

$$N_{CO_2}a \times 2\pi rH \cdot dr = G^{'} d\left(\frac{y_{co_2}}{1-y_{co_2}}\right) \quad (33)$$

where $G^{'}$ is the inlet gas flow rate without dissolution or reaction.

Eq. (34) can be obtained by combining Eq. (32) and Eq. (33):

$$K_G a \times P\left(y_{co_2} - y^*_{co_2}\right) \times 2\pi rH \cdot dr = G^{'} d\left(\frac{y_{co_2}}{1-y_{co_2}}\right) \quad (34)$$

The boundary conditions adopted in this study for the RZB are:

$$\begin{cases} r = r_i \\ r = r_o \end{cases} \qquad \begin{cases} y = y_{CO_2-in} \\ y = y_{CO_2-out} \end{cases} \quad (35)$$

where r_i and r_o are the inner and outer radius of the rotor, respectively, and y_{CO_2-in} and y_{CO_2-out} represent the molar concentration fraction of CO_2 in the gas stream entering and leaving the RZB, respectively.

Thus K_Ga can be obtained by the following expression:

$$K_Ga = \frac{G'}{\pi PH\left(r_o^2 - r_i^2\right)} \int_{y_{CO_2-in}}^{y_{CO_2-out}} \frac{1}{y_{co_2} - y_{co_2}^*} d\left(\frac{y_{co_2}}{1 - y_{co_2}}\right) \tag{36}$$

Because reactions between CO_2 and the aqueous amine solutions containing DETA, PZ and 1-MPZ are fast [37,65], the absorbed CO_2 in these solutions is consumed immediately. Therefore, $y_{co_2}^* (= mx_{CO_2})$ is close to zero and negligible, and the K_Ga values in the RZB can be calculated by Eq. (37):

$$K_Ga = \frac{G'}{\pi PH\left(r_o^2 - r_i^2\right)} \left[ln \frac{y_{CO_2-in}\left(1 - y_{CO_2-out}\right)}{y_{CO_2-out}\left(1 - y_{CO_2-in}\right)} + \left(\frac{y_{CO_2-in}}{1 - y_{CO_2-in}} - \frac{y_{CO_2-out}}{1 - y_{CO_2-out}} \right) \right] \tag{37}$$

In conventional packed columns, *HTU* is related to height of the packing and number of mass transfer unit *(NTU)* and can be calculated by the following equations [66]:

$$HTU = \frac{\text{height of the packing}}{NTU} \tag{38}$$

$$NTU = \int_{y_1}^{y_2} \frac{1}{y - y^*} dy \tag{39}$$

In the RZB, the gas and liquid phases contact countercurrently along the radial direction [57], which is similar to fluid flow in an RPB. Therefore, the *HTU* of the RZB can refer to the calculation of *HTU* in RPB [49] and be calculated as follows:

$$HTU = \frac{r_o - r_i}{NTU} \tag{40}$$

$$NTU = ln \frac{y_{CO_2-in}\left(1 - y_{CO_2-out}\right)}{y_{CO_2-out}\left(1 - y_{CO_2-in}\right)} + \left(\frac{y_{CO_2-in}}{1 - y_{CO_2-in}} - \frac{y_{CO_2-out}}{1 - y_{CO_2-out}} \right) \tag{41}$$

3. Results and discussion

3.1. Effect of promoter concentration

Fig. 4 shows the CO_2 absorption efficiency and mass transfer performance in the DETA-based solution with different promoters of various concentrations. It can be seen that both PZ and 1-MPZ could enhance the CO_2 absorption efficiency of DETA solution and mass transfer efficiency by increasing reaction rate. The promoting effect of PZ was better than that of 1-MPZ. Although 1-MPZ has similar CO_2 absorption rate with PZ at the same mole concentration [35,37], relative molecular mass of 1-MPZ (100.16) is greater than that of PZ (86.14), leading to less number of 1-MPZ molecules participating in CO_2 absorption than that of PZ when PZ and 1-MPZ have the same mass fraction. Therefore, CO_2 absorption performance of DETA + PZ solution was better than that of DETA + 1-MPZ solution. When PZ concentration exceeded 5 wt%, the CO_2 absorption percentage increased slowly.

With the rise of PZ concentration, the reaction rate constant of amine solution increases, leading to an increase in CO_2 absorption efficiency and K_Ga. However, when PZ concentration further increases, mass transfer plays a more significant role, and CO_2 absorption efficiency and K_Ga gradually reach the limitation under this operating condition in the RZB. Thus CO_2 absorption efficiency and K_Ga increased slowly when PZ concentration exceeded 5 wt% [31]. CO_2 absorption efficiency and K_Ga of DETA + 1-MPZ solution was lower than those of DETA + PZ solution and maintained linear growth because its reaction rate is lower than that of DETA + PZ solution. Due to the high cost of the promoter and the low solubility of PZ in aqueous solution [65], 5 wt% of promoter is considered as a suitable dosage in this study.

3.2. Effect of lean solution flow rate

The effect of the lean solution flow rate on CO_2 absorption efficiency, K_Ga and *HTU* is given in Fig. 5, which shows that CO_2 absorption efficiency in both DETA + PZ and DETA + 1-MPZ solutions markedly rose with an increase of the lean solution flow rate from 2 to 6 L/h, and leveled off over 6 L/h. Meanwhile, it is evident that K_Ga increased and *HTU* decreased with the rise of lean solution flow rate.

The increase of lean solution flow rate not only gives rise to a higher liquid holdup in the rotor but also enlarges the gas–liquid interface area, leading to the participation of more amine solution in CO_2 absorption. Moreover, because reactions of CO_2 with these absorbents are controlled by liquid-film, mass transfer is facilitated by higher renewal rate of gas–liquid interface with the increase of lean solution flow rate.

3.3. Effect of inlet gas flow rate

Fig. 6a shows the effect of inlet gas flow rate on CO_2 absorption efficiency in the RZB. The effect of inlet gas flow rate on CO_2 absorption efficiency was opposite to that of lean solution flow rate, exhibiting a decreasing CO_2 absorption efficiency with rising inlet gas flow rate. The DETA + PZ solution demonstrates better CO_2 absorption effect than DETA + 1-MPZ, and the difference is more pronounced at higher inlet gas flow rate. The CO_2 absorption efficiency of DETA + PZ solution reached 99.3% at an inlet gas flow rate of 1.5 m^3/h.

Fig. 6b presents the effect of inlet gas flow rate on K_Ga and *HTU*. It can be seen that K_Ga increased when inlet gas flow rate rose until 3.0 m^3/h and reduced when inlet gas flow rate was over 3.0 m^3/h. When

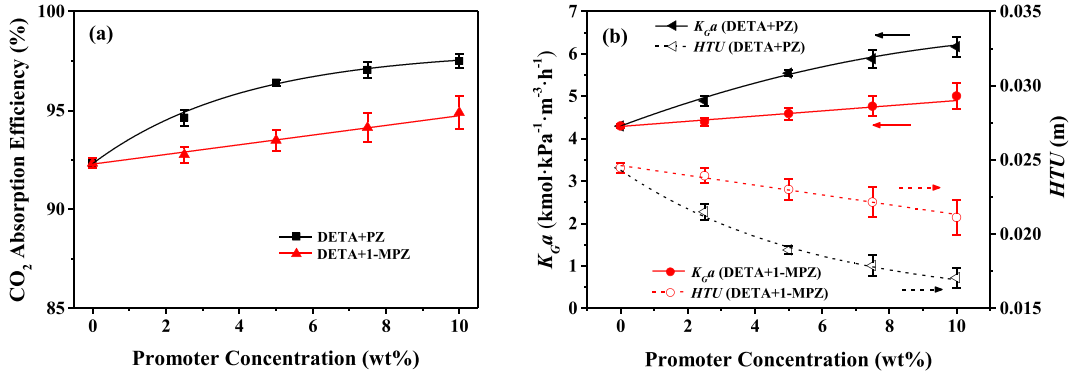

Fig. 4. Effect of promoter concentration on (a) CO_2 absorption efficiency, (b) K_Ga and *HTU* in the RZB (G = 3.0 m^3/h, L = 8 L/h, N = 1000 rpm, T = 40 °C, $T_{inlet\ gas}$ = 20 °C, C_{CO2} = 10%, C_{Amine} = 30 wt%, α = 0.03–0.04 mol/mol, one stage).

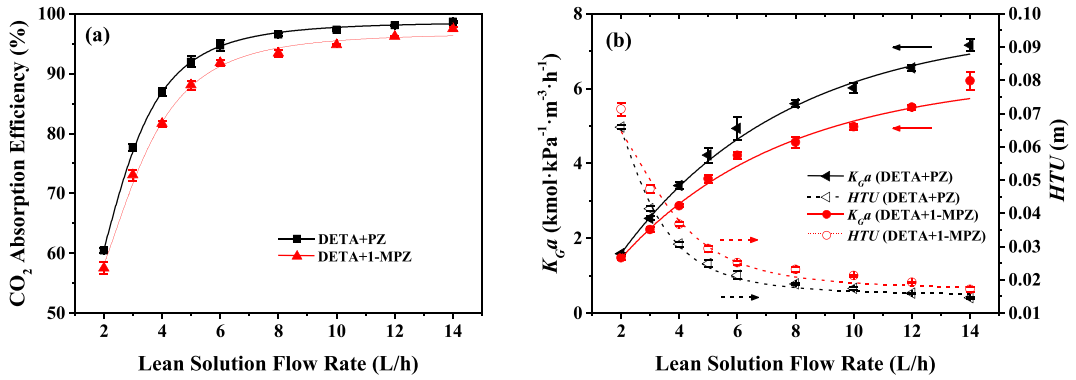

Fig. 5. Effect of lean solution flow rate on (a) CO_2 absorption efficiency, (b) K_Ga and *HTU* in the RZB ($G = 3.0$ m^3/h, $N = 1000$ rpm, $T = 40$ °C, $T_{inlet\ gas} = 20$ °C, $C_{CO2} = 10\%$, $C_{DETA} = 25$ wt%, $C_{PZ/1\text{-}MPZ} = 5$ wt%, $\alpha = 0.03$–0.04 mol/mol, one stage).

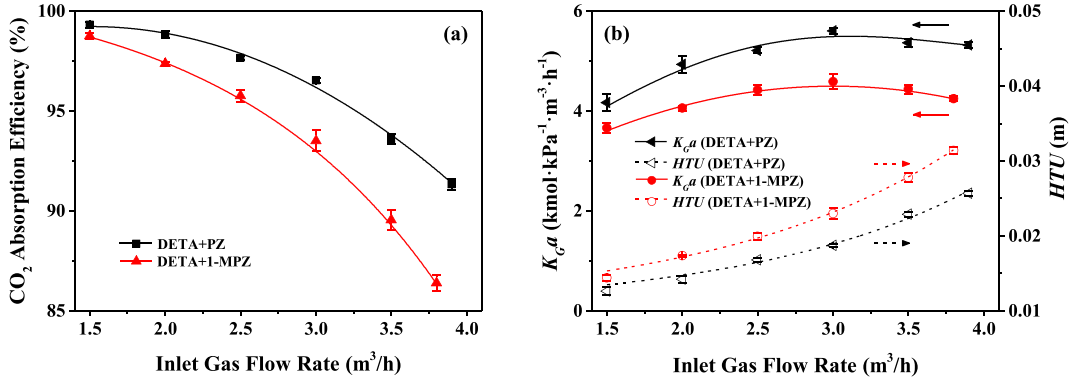

Fig. 6. Effect of inlet gas flow rate on (a) CO_2 absorption efficiency, (b) K_Ga and *HTU* in the RZB ($L = 8$ L/h, $N = 1000$ rpm, $T = 40$ °C, $T_{inlet\ gas} = 20$ °C, $C_{CO2} = 10\%$, $C_{DETA} = 25$ wt%, $C_{PZ/1\text{-}MPZ} = 5$ wt%, $\alpha = 0.03$–0.04 mol/mol, one stage).

inlet gas flow rate rises, both gas velocity and gas–liquid turbulence increase, which is conducive to the mass transfer. Meanwhile, the gas residence time decreases and an increasing amount of unabsorbed CO_2 leaves the RZB, leading to the reduction of CO_2 absorption percentage and a negative impact on K_Ga. Therefore, when the inlet gas flow rate was less than 3 m^3/h, the former factor played a leading role and brought about the increase of the mass transfer coefficient; when the inlet gas flow rate was over 3 m^3/h, the latter factor predominated, resulting in the decrease of the mass transfer coefficient. Three m^3/h was thus determined as a suitable inlet gas flow rate.

In addition, *HTU* increased with the rise of inlet gas flow rate. As *HTU* is related to CO_2 concentration of gas inlet and outlet, a decreasing CO_2 absorption efficiency thus causes an increasing *HTU* according to Eqs. (40) and (41).

3.4. Effect of rotational speed

The effect of rotational speed on CO_2 absorption efficiency, K_Ga and *HTU* is shown in Fig. 7. CO_2 absorption efficiency increased with the increase of rotational speed but gradually leveled off when the rotational speed was over 1000 rpm. With the increase of rotational speed, the shear force and centrifugal force produced by the rotation baffles rise in the RZB, causing better liquid dispersion and smaller size of droplets. Therefore, gas–liquid effective interfacial area increases and mass transfer resistance decreases, both of which are conducive to CO_2 absorption. Moreover, a rising liquid surface renewal rate in the rotor with

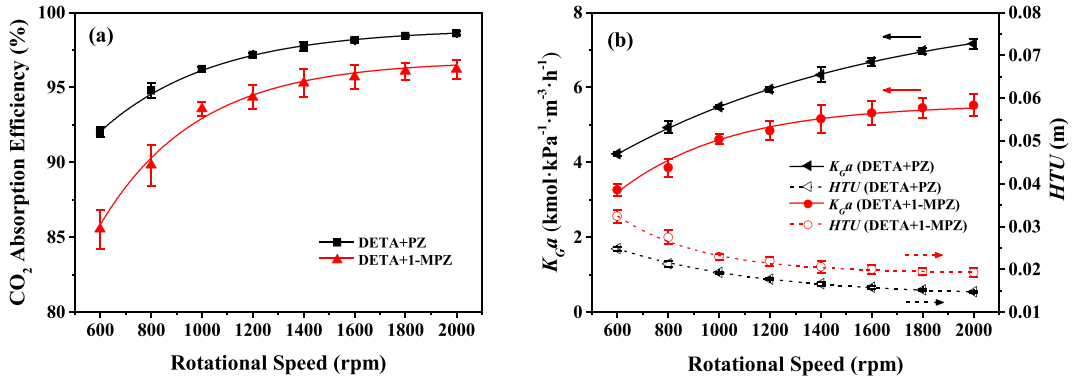

Fig. 7. Effect of rotational speed on (a) CO_2 absorption efficiency, (b) K_Ga and *HTU* in the RZB ($G = 3.0$ m^3/h, $L = 8$ L/h, $T = 40$ °C, $T_{inlet\ gas} = 20$ °C, $C_{CO2} = 10\%$, $C_{DETA} = 25$ wt%, $C_{PZ/1\text{-}MPZ} = 5$ wt%, $\alpha = 0.03$–0.04 mol/mol, one stage).

an increasing rotational speed enhances the gas–liquid mass transfer. However, the liquid residence time and holdup decrease at the same time, resulting in insufficiency of absorbents participating in CO_2 absorption, and thus CO_2 absorption efficiency increased slowly when the rotational speed exceeded 1000 rpm.

The profile of K_Ga was generally the same as that of CO_2 absorption efficiency, while *HTU* decreased with an increasing rotational speed, confirming that RZB can significantly intensify gas–liquid mass transfer in the CO_2 absorption processes.

3.5. Effect of lean solution temperature

Fig. 8 shows the variation of CO_2 absorption efficiency, K_Ga and *HTU* with rising lean solution temperature. CO_2 absorption efficiency and K_Ga increased before lean solution temperature reached 60 °C, and declined after that. However, *HTU* had an opposite variation under the same conditions. The reaction rate between CO_2 and absorbent rises with an increase in lean solution temperature. Meanwhile, the diffusion of CO_2 and amine molecules in liquid phase is enhanced and mass transfer resistance in liquid phase decreases, causing better CO_2 absorption efficiency and mass transfer performance. However, the solubility of CO_2 in the aqueous amine solution decreases and the CO_2 desorption rate also rises with an increase in lean solution temperature, which are not conducive to CO_2 absorption. In addition, a higher temperature results in a greater volatilization of absorbent, which is also unfavorable for CO_2 absorption. When lean solution temperature was less than 60 °C, the former factor played a leading role, while the latter factor predominated when lean solution temperature was over 60 °C. These factors led to extreme points of CO_2 absorption efficiency, K_Ga and *HTU* at the lean solution temperature of 60 °C. Therefore, room temperature to 60 °C is considered as an appropriate lean solution temperature range.

3.6. Effect of inlet gas CO_2 concentration

The effect of inlet gas CO_2 concentration on CO_2 absorption in the RZB is shown in Fig. 9. It can be seen that CO_2 absorption efficiency decreased with the increase of inlet gas CO_2 concentration and the tendency slowed down at higher inlet gas CO_2 concentration. The curve trend of K_Ga was similar to that of CO_2 absorption efficiency, but the profile of *HTU* was opposite to those of K_Ga and CO_2 absorption efficiency. K_Ga of the DETA + PZ solution reached 7.43 kmol/kPa m^3 h when the inlet gas CO_2 concentration was about 2%.

Because absorbent flow rate and CO_2 absorption ability are constant, a growing amount of CO_2 leaves RZB unabsorbed with a rising inlet gas CO_2 concentration, resulting in a decline of CO_2 absorption efficiency and K_Ga but a rising *HTU*. However, with the increase of inlet gas CO_2 concentration, driving force for CO_2 mass transfer between gas bulk and gas–liquid interface increases. Thus high inlet gas CO_2 concentration has insignificant effect on CO_2 absorption when the latter factor starts playing a role in the range of inlet gas CO_2 concentration of 2–10%.

3.7. Effect of CO_2 loading of lean solutions

Fig. 10a shows that the dependence of CO_2 absorption efficiency on CO_2 loading of lean solutions. It can be seen that CO_2 absorption efficiency of these two blended absorbents declined with a rising CO_2 loading. For DETA + PZ solution, the CO_2 absorption percentage remained above 80% until 0.43 mol/mol while the DETA + 1-MPZ solution exhibited the same performance below 0.34 mol/mol, suggesting that the DETA + PZ solution has greater CO_2 absorption capacity than the DETA + 1-MPZ solution at the same CO_2 loading. When CO_2 loading of absorbents increases, free amine in liquid phase is reduced, thereby causing a decreased capacity for the absorbents to accommodate CO_2. Meanwhile, the viscosity of aqueous amine solution rises with an increase in CO_2 loading, resulting in the increase of liquid phase mass transfer resistance and thus the impediment to mass transfer, as shown in Fig. 10b.

3.8. Comparison of CO_2 absorption efficiency in one stage and two stages of the RZB

Fig. 11 illustrates the comparison of the CO_2 absorption efficiency between one stage and two stages of the RZB with different lean solution flow rate. It can be seen that two stages greatly improved CO_2 absorption percentage compared to one stage. When lean solution flow rate of DETA + PZ solution reached 4L/h, CO_2 absorption efficiency in two stages attained 98%, while that in one stage was about 88%. A similar improvement was also observed with DETA + 1-MPZ solution.

For RZB, it is easy and convenient to install multiple rotors in one casing [57]. In this study, the RZB has two stages with two respective rotors. The residence and contact time of absorbents and CO_2 in the RZB increases greatly when they flow continuously through two rotors and CO_2 absorption performance is thus improved markedly.

The experimental conditions and results of CO_2 absorption in RZB is presented in Table S1 in the Supplementary Data file.

3.9. Comparison of performance between RZB and RPB

To evaluate the CO_2 absorption and mass transfer performance of the RZB, the experimental results obtained from the RZB were compared with those from an RPB with packing of stainless wire mesh [49,67]. These results are presented in Table 2.

It can be seen from Table 2 that the CO_2 absorption efficiency and K_Ga achieved in the RZB were significantly higher than those in the RPB. K_Ga in the RZB was more than two times of that in the RPB. Moreover,

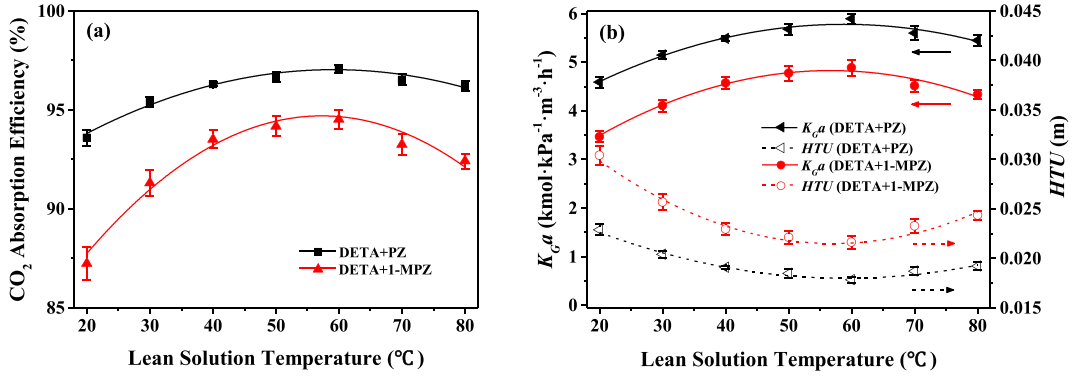

Fig. 8. Effect of lean solution temperature on (a) CO_2 absorption efficiency, (b) K_Ga and *HTU* in the RZB (G = 3.0 m^3/h, L = 8 L/h, N = 1000 rpm, $T_{inlet\ gas}$ = 20 °C, C_{CO2} = 10%, C_{DETA} = 25 wt%, $C_{PZ/1\text{-}MPZ}$ = 5 wt%, α = 0.03–0.04 mol/mol, one stage).

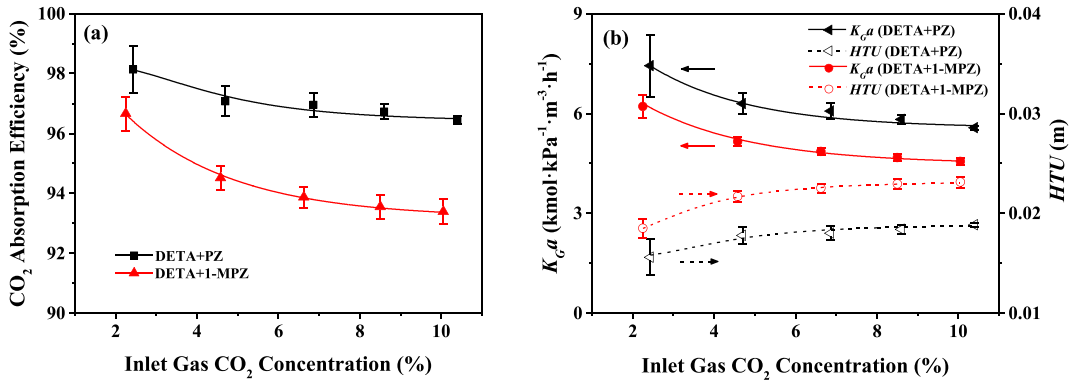

Fig. 9. Effect of inlet gas CO_2 concentration on (a) CO_2 absorption efficiency, (b) K_Ga and *HTU* in the RZB (G = 3.0 m^3/h, L = 8 L/h, N = 1000 rpm, T = 40 °C, $T_{inlet\ gas}$ = 20 °C, C_{DETA} = 25 wt%, $C_{PZ/1\text{-}MPZ}$ = 5 wt%, α = 0.03–0.04 mol/mol, one stage).

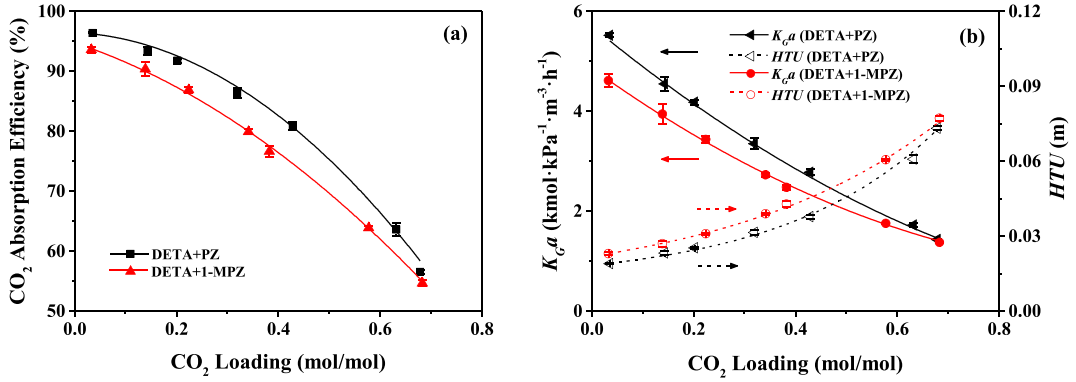

Fig. 10. Effect of CO_2 loading of lean solutions on (a) CO_2 absorption efficiency, (b) K_Ga and *HTU* in the RZB (G = 3.0 m^3/h, L = 8 L/h, N = 1000 rpm, T = 40 °C, $T_{inlet\ gas}$ = 20 °C, C_{CO2} = 10%, C_{DETA} = 25 wt%, $C_{PZ/1\text{-}MPZ}$ = 5 wt%, one stage).

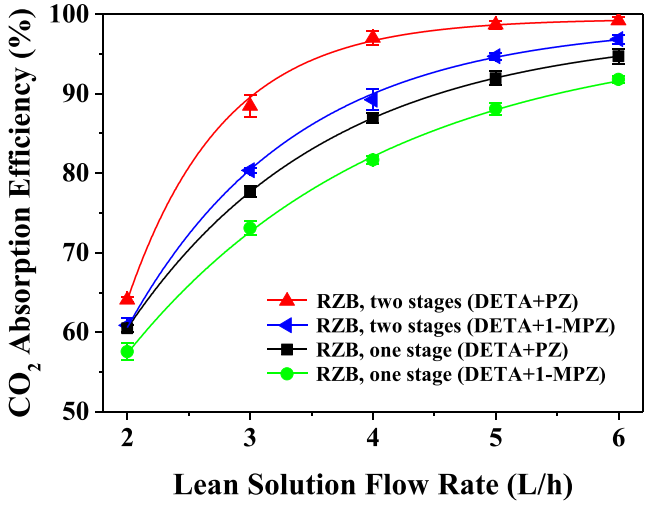

Fig. 11. Comparison CO_2 absorption efficiency in different stages of the RZB (G = 3.0 m^3/h, N = 1000 rpm, T = 40 °C, $T_{inlet\ gas}$ = 20 °C, C_{CO2} = 10%, C_{DETA} = 25 wt%, $C_{PZ/1\text{-}MPZ}$ = 5 wt%, α = 0.03–0.04 mol/mol).

the RZB has a smaller rotor volume and less absorbent consumption than the RPB. It is deduced that compared to RPB the zigzag channel structure in the RZB rotor significantly extends liquid and gas residence time and increases liquid holdup, and thus promotes the mass transfer of the CO_2-amine systems controlled by liquid film, thereby demonstrating advantages over RPB in CO_2 absorption.

Table 2
Comparison of CO_2 absorption and mass transfer performance between the RZB and the RPB.

	This work	Sheng [49,67]
Device	RZB (one stage)	RPB (stainless wire mess)
Rotor volume (cm^3)	665	833
Absorbent	25 wt% DETA + 5 wt% PZ	25 wt% DETA + 5 wt% PZ
Inlet gas flow rate (m^3/h)	1.5–3.9	1.1–3.8
Lean solution flow rate (L/h)	8	11
Rotational speed (rpm)	1000	1000
Inlet gas CO_2 concentration (%)	10	10
Lean solution temperature (°C)	40	40
CO_2 loading (mol/mol)	0.04	0.03
η (%)	91.3–99.3	72.9–94.6
K_Ga (kmol/kPa m^3 h)	4.16–5.60	1.37–2.52
HTU (m)	0.013–0.026	0.016–0.036

4. Conclusions

In this study, an RZB was used to enhance CO_2 absorption process in DETA-based solutions. The effects of various operating parameters on the CO_2 absorption efficiency, K_Ga and *HTU* were investigated. It is found that both PZ and 1-MPZ were effective promoters, while PZ exhibited better performance. CO_2 absorption efficiency increased with a rising lean solution flow rate and rotational speed, and declined with an increasing inlet gas flow rate, inlet gas CO_2 concentration and CO_2 loading of lean solutions. The highest K_Ga and CO_2 absorption efficiency were achieved at 60 °C in the lean solution temperature range of

20–80 °C. K_Ga reached the maximum value when inlet gas flow rate was 3.0 m^3/h in the gas flow rate range of 1.5–3.9 m^3/h, while the profiles of K_Ga were the same as those of CO_2 absorption efficiency in other operating conditions. In addition, the curve trend of *HTU* was opposite to that of CO_2 absorption efficiency.

Relative to one stage, two stages significantly improved the performance of the RZB on CO_2 absorption because of the extension of gas and liquid residence time and increase of liquid holdup in the RZB. Meanwhile, compared to an RPB with the stainless wire mesh packing, RZB exhibits advantage on CO_2 absorption with the DETA + PZ system, suggesting that RZB is an effective process intensification device with great potential for CO_2 absorption and may find applications where high CO_2 absorption efficiency and large turndown ratio are required in confined space.

CRediT authorship contribution statement

Zhibang Liu: Investigation, Formal analysis, Writing - original draft, Writing - review & editing. **Arash Esmaeili:** Methodology, Resources. **Hanxiao Zhang:** Validation, Data curation. **Hao Xiao:** Resources, Data curation. **Jimmy Yun:** Formal analysis, Visualization. **Lei Shao:** Conceptualization, Supervision, Funding acquisition.

Declaration of Competing Interest

The authors declare that they have no known competing financial interests or personal relationships that could have appeared to influence the work reported in this paper.

Acknowledgement

This work was supported by the National Natural Science Foundation of China (No. 21676008).

Appendix A. Supplementary data

Supplementary data to this article can be found online at https://doi.org/10.1016/j.fuel.2021.121165.

References

[1] Gatti LV, Gloor M, Miller JB, Doughty CE, Malhi Y, Domingues LG, et al. Drought sensitivity of Amazonian carbon balance revealed by atmospheric measurements. Nature 2014;506(7486):76–80.
[2] Mohanty CR, Meikap BC. Modeling the operation of a three-stage fluidized bed reactor for removing CO_2 from flue gases. J Hazard Mater 2011;187(1–3):113–21.
[3] Climate. gov. Climate Change: Atmospheric Carbon Dioxide, https://www.climate.gov/news-features/understanding-climate/climate-change-atmospheric-carbon-dioxide; 2020 [accessed 20 February 2020].
[4] Intergovernmental Panel on Climate Change (IPCC). Contribution of working group III to the fourth assessment report of the intergovernmental panel on climate change. Cambridge, United Kingdom/New York, United States: Cambridge University Press; 2007.
[5] Das D, Meikap BC. Comparison of adsorption capacity of mono-ethanolamine and di-ethanolamine impregnated activated carbon in a multi-staged fluidized bed reactor for carbon-dioxide capture. Fuel 2018;224:47–56.
[6] Das D, Meikap BC. Removal of CO_2 in a multi stage fluidised bed reactor by monoethanolamine impregnated activated carbon. Mineral Process Extractive Metall 2019;130(2):98–104.
[7] Mohanty CR, Meikap BC. Pressure drop characteristics of a multi-stage counter-current fluidized bed reactor for control of gaseous pollutants. Chem Eng Process Process Intensif 2009;48(1):209–16.
[8] Das D, Behera SK, Meikap BC. Removal of CO_2 in a multistage fluidized bed reactor by amine impregnated activated carbon: optimization using response surface methodology. Int J Coal Sci Technol 2019;6(3):445–58.
[9] Das D, Samal DP, Meikap BC. Removal of CO_2 in a multistage fluidized bed reactor by diethanol amine impregnated activated carbon. J Environ Sci Health A Tox Hazard Subst Environ Eng 2016;51(9):769–75.
[10] Akkarawatkhoosith N, Kaewchada A, Jaree A. High-throughput CO_2 capture for biogas purification using monoethanolamine in a microtube contactor. J Taiwan Inst Chem Eng 2019;98:113–23.
[11] Yin L, Li X, Zhang L, Li J. Characteristics of carbon dioxide desorption from MEA-based organic solvent absorbents. Int J Greenhouse Gas Control 2021;104.
[12] Liu H, Li M, Idem R, Tontiwachwuthikul P, Liang Z. Analysis of solubility, absorption heat and kinetics of CO_2 absorption into 1-(2-hydroxyethyl)pyrrolidine solvent. Chem Eng Sci 2017;162:120–30.
[13] Zhang P, Xu R, Li H, Gao H, Liang Z. Mass transfer performance for CO_2 absorption into aqueous blended DMEA/MEA solution with optimized molar ratio in a hollow fiber membrane contactor. Sep Purif Technol 2019;211:628–36.
[14] Fan W, Liu Y, Wang K. Detailed experimental study on the performance of Monoethanolamine, Diethanolamine, and Diethylenetriamine at absorption/regeneration conditions. J Cleaner Prod 2016;125:296–308.
[15] Muchan P, Narku-Tetteh J, Saiwan C, Idem R, Supap T. Effect of number of amine groups in aqueous polyamine solution on carbon dioxide (CO_2) capture activities. Sep Purif Technol 2017;184:128–34.
[16] Pandey D, Mondal MK. Equilibrium CO_2 solubility in the aqueous mixture of MAE and AEEA: Experimental study and development of modified thermodynamic model. Fluid Phase Equilib 2020;522.
[17] Wai SK, Nwaoha C, Saiwan C, Idem R, Supap T. Absorption heat, solubility, absorption and desorption rates, cyclic capacity, heat duty, and absorption kinetic modeling of AMP–DETA blend for post–combustion CO_2 capture. Sep Purif Technol 2018;194:89–95.
[18] Hartono A, da Silva EF, Svendsen HF. Kinetics of carbon dioxide absorption in aqueous solution of diethylenetriamine (DETA). Chem Eng Sci 2009;64(14):3205–13.
[19] Fu K, Sema T, Liang Z, Liu H, Na Y, Shi H, et al. Investigation of Mass-Transfer Performance for CO_2 Absorption into Diethylenetriamine (DETA) in a Randomly Packed Column. Ind Eng Chem Res 2012;51(37):12058–64.
[20] Zhang X, Fu K, Liang Z, Rongwong W, Yang Z, Idem R, et al. Experimental studies of regeneration heat duty for CO_2 desorption from diethylenetriamine (DETA) solution in a stripper column packed with Dixon ring random packing. Fuel 2014;136:261–7.
[21] Bernhardsen IM, Knuutila HK. A review of potential amine solvents for CO_2 absorption process: Absorption capacity, cyclic capacity and pKa. Int J Greenhouse Gas Control 2017;61:27–48.
[22] Choi SY, Nam SC, Yoon YI, Park KT, Park S-J. Carbon dioxide absorption into aqueous blends of methyldiethanolamine (MDEA) and alkyl amines containing multiple amino groups. Ind Eng Chem Res 2014;53(37):14451–61.
[23] Liu J, Li X, Zhang Z, Li L, Bi Y, Zhang L. Promotion of CO_2 capture performance using piperazine (PZ) and diethylenetriamine (DETA) bi-solvent blends. Greenhouse Gases Sci Technol 2019;9(2):349–59.
[24] Chang Y-C, Leron RB, Li M-H. Equilibrium solubility of carbon dioxide in aqueous solutions of (diethylenetriamine+piperazine). J Chem Thermodyn 2013;64:106–13.
[25] Joseph EB, Vaidya PD. Kinetics of CO_2 absorption by aqueous mixtures of N, N′-diethylethanolamine and polyamines. Int J Chem Kinet 2019;51(2):131–7.
[26] Nwaoha C, Saiwan C, Supap T, Idem R, Tontiwachwuthikul P, Rongwong W, et al. Carbon dioxide (CO_2) capture performance of aqueous tri-solvent blends containing 2-amino-2-methyl-1-propanol (AMP) and methyldiethanolamine (MDEA) promoted by diethylenetriamine (DETA). Int J Greenhouse Gas Control 2016;53:292–304.
[27] Orhan OY, Alper E. Kinetics of carbon dioxide binding by promoted organic liquids. Chem Eng Technol 2015;38(8):1485–9.
[28] Borhani NT, Wang M. Role of solvents in CO2 capture processes: The review of selection and design methods. Renewable Sustainable Energy Rev 2019;114.
[29] Sheng M, Xie C, Zeng X, Sun B, Zhang L, Chu G, et al. Intensification of CO_2 capture using aqueous diethylenetriamine (DETA) solution from simulated flue gas in a rotating packed bed. Fuel 2018;234:1518–27.
[30] Wu T-W, Hung Y-T, Chen M-T, Tan C-S. CO_2 capture from natural gas power plants by aqueous PZ/DETA in rotating packed bed. Sep Purif Technol 2017;186:309–17.
[31] Zhan J, Wang B, Zhang L, Sun B-C, Fu J, Chu G-w, et al. Simultaneous absorption of H_2S and CO_2 into the MDEA + PZ aqueous solution in a rotating packed bed. Ind Eng Chem Res 2020;59(17):8295–303.
[32] Lin C-C, Chen Y-W. Performance of a cross-flow rotating packed bed in removing carbon dioxide from gaseous streams by chemical absorption. Int J Greenhouse Gas Control 2011;5(4):668–75.
[33] Samanta A, Bandyopadhyay SS. Absorption of carbon dioxide into aqueous solutions of piperazine activated 2-amino-2-methyl-1-propanol. Chem Eng Sci 2009;64(6):1185–94.
[34] Conway W, Wang X, Fernandes D, Burns R, Lawrance G, Puxty G, et al. Toward rational design of amine solutions for PCC applications: the kinetics of the reaction of CO_2 (aq) with cyclic and secondary amines in aqueous solution. Environ Sci Technol 2012;46(13):7422–9.
[35] Li H, Le Moullec Y, Lu J, Chen J, Valle Marcos JC, Chen G, et al. CO_2 solubility measurement and thermodynamic modeling for 1-methylpiperazine/water/CO_2. Fluid Phase Equilib 2015;394:118–28.
[36] Rayer AV, Sumon KZ, Henni A, Tontiwachwuthikul P. Kinetics of the reaction of carbon dioxide (CO_2) with cyclic amines using the stopped-flow technique. Energy Procedia 2011;4:140–7.
[37] Chen X, Rochelle GT. Aqueous piperazine derivatives for CO_2 capture: accurate screening by a wetted wall column. Chem Eng Res Des 2011;89(9):1693–710.
[38] Rayer AV, Armugam Y, Henni A, Tontiwachwuthikul P. High-pressure solubility of carbon dioxide (CO_2) in aqueous 1-methyl piperazine solution. J Chem Eng Data 2014;59(11):3610–23.
[39] Khalili F, Rayer AV, Henni A, East ALL, Tontiwachwuthikul P. Kinetics and dissociation constants (pKa) of polyamines of importance in post-combustion carbon dioxide (CO_2) capture studies. Recent advances in post-combustion CO_2 capture. Chemistry 2012:43–70.

[40] Wang Z, Yang T, Liu Z, Wang S, Gao Y, Wu M. Mass transfer in a rotating packed bed: a critical review. Chem Eng Process Process Intensif 2019;139:78–94.
[41] Zou H, Sheng M, Sun X, Ding Z, Arowo M, Luo Y, et al. Removal of hydrogen sulfide from coke oven gas by catalytic oxidative absorption in a rotating packed bed. Fuel 2017;204:47–53.
[42] Wang D, Liu T, Ma L, Wang F, Shao L. Modeling and experimental studies on ozone absorption into phenolic solution in a rotating packed bed. Ind Eng Chem Res 2019;58(17):7052–62.
[43] Wenzel D, Górak A. Review and analysis of micromixing in rotating packed beds. Chem Eng J 2018;345:492–506.
[44] Sang L, Luo Y, Chu G-W, Liu Y-Z, Liu X-Z, Chen J-F. Modeling and experimental studies of mass transfer in the cavity zone of a rotating packed bed. Chem Eng Sci 2017;170:355–64.
[45] Borhani TN, Oko E, Wang M. Process modelling and analysis of intensified CO_2 capture using monoethanolamine (MEA) in rotating packed bed absorber. J Cleaner Prod 2018;204:1124–42.
[46] Sang L, Luo Y, Chu GW, Sun BC, Zhang LL, Chen JF. A three-zone mass transfer model for a rotating packed bed. AIChE J 2019;65(6).
[47] Wu S, Zhang L, Sun B, Zou H, Zeng X, Luo Y, et al. Mass-transfer performance for CO_2 absorption by 2-(2-aminoethylamino)ethanol solution in a rotating packed bed. Energy Fuels 2017;31(12):14053–9.
[48] Zhang W, Xie P, Li Y, Teng L, Zhu J. Hydrodynamic characteristics and mass transfer performance of rotating packed bed for CO_2 removal by chemical absorption: a review. J Nat Gas Sci Eng 2020;79.
[49] Sheng M, Sun B, Zhang F, Chu G, Zhang L, Liu C, et al. Mass-transfer characteristics of the CO_2 absorption process in a rotating packed bed. Energy Fuels 2016;30(5):4215–20.
[50] Guo K, Guo F, Feng Y, et al. Synchronous visual and RTD study on liquid flow in rotating packed-bed contactor. Chem Eng Sci 2000;55:1699–706.
[51] Sheng M, Liu C, Ge C, Arowo M, Xiang Y, Sun B, et al. Mass-transfer performance of CO_2 absorption with aqueous diethylenetriamine-based solutions in a packed column with dixon rings. Ind Eng Chem Res 2016;55(40):10788–93.
[52] Wang GQ, Zhou ZJ, Li YM, Ji JB. Qualitative relationships between structure and performance of rotating zigzag bed in distillation. Chem Eng Proces Process Intensif 2019;135:141–7.
[53] Li Y, Liu P, Wang G, Ji J. Enhanced mass transfer and reduced pressure drop in a compound rotating zigzag bed. Sep Purif Technol 2020;250.
[54] Karmakar S, Bhowal A, Das P. A comparative study of liquid-liquid extraction in different rotating bed contactors. Chem Eng Process Process Intensif 2018;132:187–93.
[55] Liang Z, Wei T, Xie J, Li H, Liu H. Direct conversion of terminal alkenes to aldehydes via ozonolysis reaction in rotating zigzag bed. J Iran Chem Soc 2020;17(9):2379–84.
[56] Li Y, Lu Y, Liu X, Wang G, Nie Y, Ji J. Mass-transfer characteristics in a rotating zigzag bed as a Higee device. Sep Purif Technol 2017;186:156–65.
[57] Wang GQ, Xu ZC, Yu YL, Ji JB. Performance of a rotating zigzag bed—a new HIGEE. Chem Eng Process Process Intensif 2008;47(12):2131–9.
[58] Li Y, Li X, Wang Y, Chen Y, Ji J, Yu Y, et al. Distillation in a counterflow concentric-ring rotating bed. Ind Eng Chem Res 2014;53(12):4821–37.
[59] Das D, Samal DP, Mohammad N, Meikap BC. Hydrodynamics of a multi-stage counter-current fluidized bed reactor with down-comer for amine impregnated activated carbon particle system. Adv Powder Technol 2017;28(3):854–64.
[60] Mohanty C, Adapala S, Meikap BC. Hold-up characteristics of a novel gas–solid multistage fluidized bed reactor for control of hazardous gaseous effluents. Chem Eng J 2009;148(1):115–21.
[61] Hu XE, Yu Q, Barzagli F, Ce L, Fan M, Gasem KAM, et al. NMR techniques and prediction models for the analysis of species formed in CO_2 capture processes with amine-based sorbents: a critical review. ACS Sustainable Chem Eng 2020;8(16):6173–93.
[62] Kim YE, Choi JH, Nam SC, Yoon YI. CO_2 absorption capacity using aqueous potassium carbonate with 2-methylpiperazine and piperazine. J Ind Eng Chem 2012;18(1):105–10.
[63] Sutar PN, Vaidya PD, Kenig EY. Activated DEEA solutions for CO_2 capture—a study of equilibrium and kinetic characteristics. Chem Eng Sci 2013;100:234–41.
[64] Pinar Gordesli FEA. The kinetics of carbon dioxide capture by solutions of piperazine and N-methyl piperazine. Int J Global Warming 2011;3:67–76.
[65] Wang M, Joel AS, Ramshaw C, Eimer D, Musa NM. Process intensification for post-combustion CO_2 capture with chemical absorption: a critical review. Appl Energy 2015;158:275–91.
[66] Ivanov IV, Lotkhov VA, Moiseeva KA, Kulov NN. Mass transfer in a packed extractive distillation column. Theor Found Chem Eng 2016;50(5):667–77.
[67] Sheng M. Study on mixed absorption solutions and technologies for CO_2 absorption [Master Thesis]. Beijing, China: Beijing University of Chemical Technology; 2015.